High-efficiency entangled photon pair collection in type-II parametric fluorescence

Christian Kurtsiefer,[1] Markus Oberparleiter,[1] and Harald Weinfurter[1,2]
[1]*Sektion Physik, Ludwig-Maximilians-Universität, D-80797 München, Germany*
[2]*Max-Planck-Institut für Quantenoptik, D-85748 Garching, Germany*
(Received 19 December 2000; published 2 July 2001)

We report on a method for optimizing the collection of entangled photon pairs in type-II parametric fluorescence. With this technique, we detected 360 000 polarization-entangled photon pairs per second in the near-ir region in single-mode optical fibers. The entanglement of the photon pairs was verified by measuring polarization correlations in different bases of at least 96%.

DOI: 10.1103/PhysRevA.64.023802 PACS number(s): 42.65.Yj, 42.50.Dv

Experiments with entangled photon pairs have opened a whole field of research. Created initially by electron-positron annihilation and later in atomic cascade decays, entangled photons allowed a distinctive comparison of various concepts of quantum mechanics [1,2]. More recently, parametric fluorescence (downconversion) in nonlinear optical crystals as the source of entangled photon pairs [3–5] led to a dramatic increase in count rates. This enabled a variety of experiments on the foundations of quantum mechanics [6–8] and the experimental realization of new concepts in quantum information [9–11]. In spite of that success, most of the experiments and potential applications still suffer from the low yield of the fluorescence process. It was thus the motivation for the work presented here to optimize collection efficiency and thereby the available rate of polarization-entangled photon pairs from parametric downconversion.

In type-II parametric fluorescence, a pump photon with energy $\hbar\omega_p$ is converted in a nonlinear optical crystal into two orthogonally polarized photons, signal and idler, obeying energy and momentum conservation. For a fixed pump photon momentum and a given idler frequency ω_i, there is a one-dimensional manifold of emission directions for the idler photon, and a corresponding one for the signal photon with a frequency ω_s with $\omega_p=\omega_i+\omega_s$, forming two emission cones. To generate polarization-entangled photon pairs, the orientation of the nonlinear crystal is chosen such that the two cones intersect. This intersection defines two directions along which the polarization of each emitted photon is undefined, but perfectly anticorrelated with the polarization of the other one. Provided complete indistinguishability of which photon belongs to which emission cone, a polarization-entangled pair of photons is obtained [5].

In most of the experiments performed, the photons have been collected into spatial modes defined by apertures, and the spectrum of the collected light has been defined with optical filters to a given bandwidth $\Delta\lambda$ around the wavelengths λ_i and λ_s of signal and idler photons. Yet, in many interferometric experiments requiring a well-defined spatial mode or for transport over larger distances, it is desirable to couple the light from the parametric downconversion into single-mode optical fibers. With specific design criteria in an experiment testing Bell inequalities with spacelike separated observers [12], typical pair rates of 13 000 s^{-1} for $\Delta\lambda_{\mathrm{FWHM}}=3$ nm at a pump power of 400 mW have been achieved (crystal thickness 3 mm) [13]. The collection efficiency there was already an order of magnitude higher than in the initial experiments using type-II downconversion sources [5]. Different techniques have been implemented since then to increase the number of entangled photon pairs emitted in a single spatial mode, including the use of two type-I conversion crystals [14], focusing the pump beam [15,16], or using resonant enhancement [17,18]. Quite recently, several groups have succeeded in designing photon pair sources with confining waveguides in periodically poled crystal structures [19,20], showing unprecedented efficiencies in the generation of correlated photon pairs. However, to our knowledge, no entangled photons have been observed with this technique yet.

Here, we present a simple way to optimize the collection efficiency, using the fixed relation between emission direction and wavelength for a fixed pump frequency. The idea is to match the angular distribution of the parametric fluorescence light for a given spectral bandwidth to the angular width of the spatial mode collected into a single-mode optical fiber. Applying this design criterion, which also can be combined with the new methods mentioned above, we achieved unprecedented coupling efficiencies and photon pair detection rates.

To optimize collection efficiency, we consider the wavelength dependency of the opening angles of the emission cones. For a given spectral width $\Delta\lambda_i=\Delta\lambda_s$, the signal and idler light emitted along the intersection directions is dispersed over an angular width $\Delta\alpha_i$ and $\Delta\alpha_s$, respectively. We use the approximate rotational symmetry of the emission cones and obtain

$$\Delta\alpha_i=\Delta\alpha_s\approx\Delta\theta_s=\Delta\theta_i=\frac{d\theta_i}{d\lambda_i}\Delta\lambda_i, \tag{1}$$

where θ_s and θ_i are the emission angles between the pump direction and signal and idler light, respectively, in a plane containing the optical axis of the (uniaxial) crystal [see the rings of intersection with a plane normal to the pump beam in Fig. 1(a)]. This expression can be obtained from energy and momentum conservation in a closed form, although the numerical solution is faster. The pump light is considered as a plane wave propagating with an angle θ_p with respect to the optical axis of the nonlinear crystal. A more detailed discussion of the relation between spectral and angular distribution of the downconverted light can be found in [22].

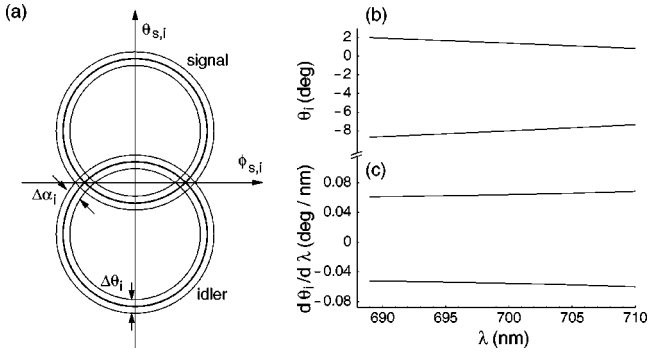

FIG. 1. (a) Geometry for the emission of signal and idler photons for a finite bandwidth. (b) Emission angle θ_i of idler relative to the pump beam for $\Theta_p = 49.7°$ and $\phi_i = 0°$. (c) Derivative $d\theta_i/d\lambda$ to estimate the angular width $\Delta\alpha_i$ to be collected.

For an appropriate choice of the crystal orientation, the two directional manifolds of signal and idler light intersect perpendicularly. Then, for a Gaussian spectral distribution of the light to be collected, the corresponding angular distributions are also Gaussian with characteristic widths $\Delta\alpha_s = \Delta\alpha_i$, and have rotational symmetry around the intersection directions. We now define Gaussian target modes aligned with the intersection directions of the emission cones with a divergence $\theta_D = \Delta\alpha_{s,i}$, which can be mapped optically to the collecting fibers. The beam waist of these Gaussian modes is given by $w_0 = \lambda/(\pi\theta_D)$. As the mode matching for the parametric downconversion is described in a plane-wave basis, we locate the waist of this Gaussian mode in the conversion crystal, as sketched in Fig. 2(a). For our configurations, the crystal is always shorter than the Rayleigh length $z_r = \pi w_0^2/\lambda$ of the corresponding modes, thus we neglect possible effects due to wavefront curvature in the conversion crystal.

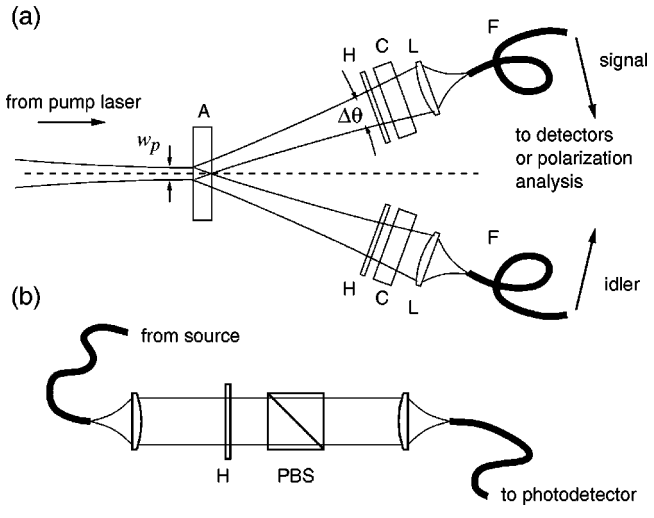

FIG. 2. Basic setup: (a) An uv pump laser beam is focused into a BBO crystal A to a waist w_p; light emitted by parametric fluorescence is mapped to the receiving modes of single-mode optical fibers F with lenses L. A combination of half-wave plates H and additional BBO crystals C is used to compensate for walkoff in the first crystal. (b) Polarization analysis in each arm with an additional half-wave plate H selecting the measurement basis and a polarizing beam splitter PBS.

Having chosen the target modes, we only collect photons being created in a region of overlap between target modes and pump field. Therefore, the pump field can be restricted to a region where the target modes have a significant field strength. To maximize overlap with the Gaussian pump field, we choose its waist w_p to be equal to the waist of the target modes in the crystal.

As in previous work [5], we use an argon-ion laser in our experiment at a wavelength of $\lambda_p = 351.1$ nm to pump a beta-barium-borate (BBO) nonlinear optical crystal (thickness 2 mm), yielding downconverted photon pairs efficiently detectable with Si avalanche diodes.

The two cones of signal and idler light at the degenerate wavelength $\lambda_s = \lambda_i = 702.2$ nm intersect perpendicularly for a pump beam orientation of $\Theta_p = 49.7°$ with respect to the optical axis, resulting in an (external) angle of $\phi_{s,i} = \pm 3.1°$ with respect to the pump beam [Fig. 1(a)].

Figures 1(b) and 1(c) show both the emission angles θ_i, θ_s and their derivatives for that configuration. The results are obtained numerically, with refractive indices of the crystal given by numerical Sellmeier equations [23]. The angles include the refraction on the crystal surfaces, assuming the crystal faces oriented normal to the pump beam direction. At a degeneracy wavelength of $\lambda = 702.2$ nm, we obtain an angular derivative of $|d\theta_i/d\lambda_i| = |d\theta_s/d\lambda_s| \approx 0.055°/\text{nm}$.

Using the asymptotic expression

$$I(\theta) \propto \exp(-2\theta^2/\theta_D^2) \tag{2}$$

for the intensity distribution $I(\theta)$ in a Gaussian target mode, and aiming for a spectral width of $\Delta\lambda_{\text{FWHM}} = 4$ nm for the downconverted photons, one would expect a divergence angle of

$$\theta_D \approx (\Delta\lambda_{\text{FWHM}}/\sqrt{2\ln 2})|d\theta_i/d\lambda_i| = 0.186°. \tag{3}$$

To compensate for an additional divergence due to the angular distribution in the pump beam, we have chosen a divergence angle $\theta_D = 0.16°$ for the target modes, corresponding to a Gaussian beam waist of $w_0 = 82$ μm. These modes were geometrically mapped with aspheric lenses ($f = 11$ mm) to the receiving modes of single-mode optical fibers with a Gaussian waist parameter determined to be $w_f = 2.3$ μm.

Transverse and longitudinal walk-off in the conversion crystal were compensated in the usual way [5] with additional polarization rotators and BBO crystals of length 1 mm to obtain polarization-entangled photons for all wavelengths in the acceptance spectrum of the downconverted light [Fig. 2(a)]. In our arrangement, we used interference filters for bandwidth selection in front of the couplers only for an initial alignment; the experimental data described below were obtained without these filters.

Figure 3 shows the spectral distribution of the converted light collected into the single-mode fibers. The spectra in both arms exhibit an almost Gaussian distribution with a full width at half maximum (FWHM) of 4.06 nm and 4.60 nm,

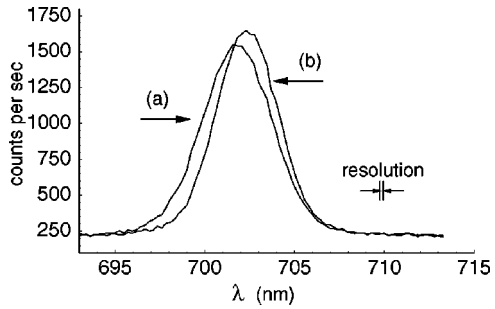

FIG. 3. Optical spectra of light collected from the downconversion into the two single-mode fibers. The spectra show a FWHM of 4.60 nm (a) and 4.06 nm (b) and are centered around the degeneracy wavelength of 702.2 nm with a separation of 0.55 nm.

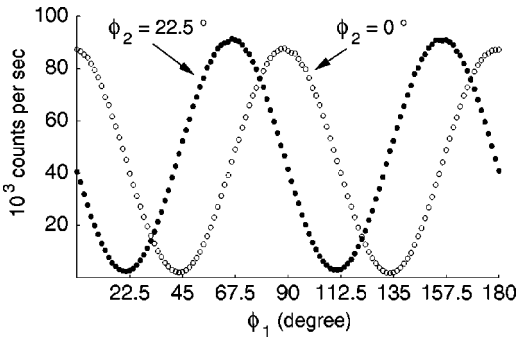

FIG. 5. Polarization correlation experiment: Coincidence count rates of the polarization analysis setup for different orientation angles ϕ_1, ϕ_2 of the half-wave plates. Uncorrected polarization correlation in the (H,V) basis is 96%, and 95% in the $\pm 45°$ basis.

respectively [24]. They are centered around the degeneracy wavelength of 702.2 nm, with a separation of 0.55 nm due to residual misalignment of the fiber coupler positions. The widths of the observed spectra are in good agreement with the estimation given above.

To determine the collection efficiency, we connected the single-mode optical fibers directly to two actively quenched silicon avalanche diodes. Figure 4 shows the coincidence count rates and the count rates for the individual detection events as a function of uv pump power. We determined a coincidence/single count ratio (i.e., an overall efficiency) of 0.286 ± 0.001 for the whole range of pump power. The maximum coincidence count rate we observed was 360 800 s^{-1} at a pump power of $P = 465$ mW [21]. The coincidence time window was measured to be $\tau_c = 6.8 \pm 0.1$ ns, thus accidental coincidence count rates being small over the whole range of pump power. For the low power regime, we obtain a slope of 900 coincidence counts per second and mW for our 2-mm-long BBO crystal in the single-mode optical fibers.

We would like to point out that the coincidence/single count ratio may significantly be affected by transverse walkoff of the extraordinary beam: The transverse walkoff for the passage through the downconversion crystal is 170 μm, which has to be compared to a receiving waist of 82 μm. For experiments requiring even higher coincidence/single count ratio, e.g., in the attempt of closing the detector loophole in an Einstein-Podolsky-Rosen (EPR) experiment, one would choose a smaller optical bandwidth, causing a larger beam waist of the target mode and thereby a less dramatic influence of the transverse walkoff. Another possibility would be the use of cylindrical lenses.

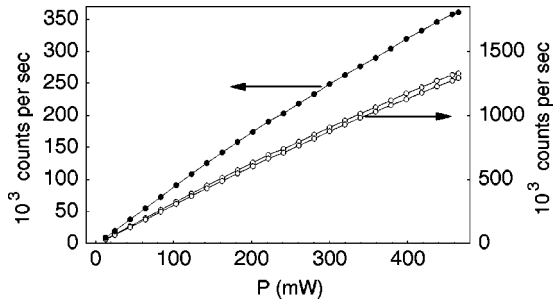

FIG. 4. Coincidence count rates (left axis) and individual count rates (right axis) of two photodetectors connected directly to the single-mode fibers as a function of uv power.

To verify the entanglement of the photon pairs obtained with this collection arrangement, we measured the polarization correlation between the photons of each pair using a polarization analyzer as shown in Fig. 2(b) formed by a half-wave plate and a polarizing beam splitter. The birefringence of the optical fiber was compensated with a ''bat ear'' polarization controller such that less than 1% of intensity was transfered from 0° or 45° linear polarization to the corresponding orthogonal polarization. After polarization analysis, the light was coupled into a multimode optical fiber, and detected by the two actively quenched silicon avalanche diodes.

The single and coincidence count rates for different orientations ϕ_1, ϕ_2 of the half-wave plates in the analyzers are shown in Fig. 5 for a uv pump power of 400 mW. For a setting of $\phi_2 = 0°$, corresponding to detecting horizontally polarized photons, we observed a visibility of the polarization correlation of $96.0 \pm 0.1\%$. This value was obtained from a sin/cos fit to the experimentally obtained coincidence count rates. To correct for accidental coincidences, we subtract a coincidence rate of $n_c = n_s n_i \tau_c (1 - \eta)$, with a total detection efficiency $\eta = 0.214$ in the polarization analysis setup, and single count rates of $n_s, n_i \approx 420\,000$ counts per second. With that, we find a visibility of $98.2 \pm 0.1\%$. For a setting of $\phi_2 = 22.5°$ corresponding of a detection of $+45°$ linearly polarized photons in arm 2, the coincidence count rate as a function of the tilt angle ϕ_1 is shown in Fig. 5. From this measurement, we obtain a bare visibility of $94.5 \pm 0.1\%$ for the polarization correlation, and $96.3 \pm 0.1\%$ after correction for accidentals. The corrected visibilities of the polarization correlation both in an (H,V) and a $(+45°, -45°)$ basis are compatible with values of $98.8 \pm 0.2\%$ and $97.0 \pm 0.2\%$ we obtained at a lower pump power of $P = 123$ mW, where accidental coincidences are negligible. Using (raw) data from the high-intensity experiment for the evaluation of a Clauser-Horne-Shimong-Holt (CHSH)-type Bell inequality, we obtain $S = -2.6979 \pm 0.0034$, i.e., a violation of 204 standard deviations for a measurement time of 1 s per angle setting.

To summarize, we presented a technique to optimize the collection of entangled photon pairs created in a type-II parametric fluorescence process using mode-matching procedures. We were thereby able to increase pair collection efficiencies of earlier experiments [13] into single-mode optical fibers by a factor of ≈ 25, supplying a strong source for quantum information experiments having attracted attention recently. It is particularly interesting to combine these techniques with resonant enhancement techniques [18], since this leads to strong sources for polarization-entangled photon pairs without the need for costly large-frame lasers [25].

We would like to acknowledge the uncomplicated help of H. Zbinden and N. Gisin from the University of Geneva with actively quenched photodetectors. This work was supported by the European Union in the FET/QuComm research project (IST-1999-10033) and the Deutsche Forschungsgemeinschaft.

[1] J. F. Clauser and A. Shimony, Rep. Prog. Phys. **41**, 1981 (1978).
[2] A. Aspect, P. Grangier, and G. Roger, Phys. Rev. Lett. **47**, 460 (1981); **49**, 91 (1982); A. Aspect, J. Dalibard, and R. Roger, *ibid.* **49**, 1804 (1982).
[3] C. K. Hong and L. Mandel, Phys. Rev. A **31**, 2409 (1985).
[4] J. G. Rarity and P. R. Tapster, Phys. Rev. Lett. **64**, 2495 (1990).
[5] P. G. Kwiat, K. Mattle, H. Weinfurter, A. Zeilinger, A. V. Sergienko, and Y. Shih, Phys. Rev. Lett. **75**, 4337 (1995).
[6] L. Mandel, Rev. Mod. Phys. **71**, S274 (1999).
[7] A. Zeilinger, Rev. Mod. Phys. **71**, S288 (1999).
[8] A. E. Steinberg, P. G. Kwiat, and R. Y. Chiao, in *Atomic, Molecular and Optical Physics Handbook*, edited by G. Drake (AIP Press, New York, 1996), Chap. 77, p. 901.
[9] D. Bouwmeester, J.-W. Pan, K. Mattle, M. Eibl, H. Weinfurter, and A. Zeilinger, Nature (London) **390**, 576 (1997).
[10] D. Bouwmeester, J.-W. Pan, M. Daniell, H. Weinfurter, and A. Zeilinger, Phys. Rev. Lett. **82**, 1345 (1999).
[11] H. Weinfurter, Adv. At., Mol., Opt. Phys. **42**, 489 (2000).
[12] G. Weihs, T. Jennewein, C. Simon, H. Weinfurter, and A. Zeilinger, Phys. Rev. Lett. **81**, 5039 (1998).
[13] G. Weihs, Ph.D. thesis, University of Vienna, 1999.
[14] P. G. Kwiat, E. Waks, A. G. White, I. Appelbaum, and P. H. Eberhard, Phys. Rev. A **60**, R773 (1999).
[15] C. H. Monken, P. H. Suoto Ribeiro, and S. Pádua, Phys. Rev. A **57**, R2267 (1998).
[16] C. H. Monken, P. H. Suoto Riberio, and S. Pádua, Phys. Rev. A **57**, 3123 (1998).
[17] Z. Y. Ou and Y. J. Lu, Phys. Rev. Lett. **83**, 2556 (1999).
[18] M. Oberparleiter and H. Weinfurter, Opt. Commun. **183**, 133 (2000).
[19] S. Tanzilli, H. de Riedmatten, W. Tittel, H. Zbinden, P. Baldi, M. de Micheli, D.B. Ostrowski, and N. Gisin, Electron. Lett. **37**, 26 (2001).
[20] K. Sanaka, K. Kawahara, and T. Kuga, e-print quant-ph/0012028.
[21] To avoid saturation effects in the counter electronics, we used a fast $\div 16$ prescaler for both single and coincidence counts.
[22] M. H. Rubin, Phys. Rev. A **54**, 5349 (1996).
[23] D. Eimerl, L. Davis, S. Velsko, E. K. Graham, and A. Zalkin, J. Appl. Phys. **62**, 1968 (1987).
[24] The resolution of the spectrometer was measured with a He-Ne reference laser to be $\Delta\lambda_{\mathrm{FWHM}} = 0.2$ nm.
[25] J. Volz, diploma thesis, University of Munich (2000).